Acta Oceanol. Sin., 2017, Vol. 36, No. 2, P. 94–104
DOI: 10.1007/s13131-017-0980-8
http://www.hyxb.org.cn
E-mail: hyxbe@263.net

Characterization of uncultivated magnetotactic bacteria from the sediments of Yuehu Lake, China

DU Haijian[1, 2†], ZHANG Rui[1, 2†], ZHANG Wenyan[1, 2], XU Cong[1, 2, 5], CHEN Yiran[1, 2], PAN Hongmiao[1, 2], ZHOU Ke[3], WU Long-fei[4], XIAO Tian[1, 2*]

[1] Key Laboratory for Marine Ecology and Environmental Sciences, Institute of Oceanology, Chinese Academy of Sciences, Qingdao 266071, China

[2] Laboratory for Marine Ecology and Environmental Science, Qingdao National Laboratory for Marine Science and Technology, Qingdao 266071, China

[3] College of Resources and Environment, Qingdao Agriculture University, Qingdao 266109, China

[4] Aix Marseille Université, CNRS, LCB UMR 7257, Institut de Microbiologie de la Méditerranée, Marseille F-13402, France

[5] University of Chinese Academy of Sciences, Beijing 100049, China

Received 4 November 2015; accepted 23 August 2016

Abstract

Marine magnetotactic bacteria were collected from the intertidal sediments of Yuehu Lake (China), where their abundance reached 10^3–10^4 ind./cm^3. Diverse morphotypes of magnetotactic bacteria were observed, including cocci and oval, vibrio-, spirillum-, rod-, elliptical-, handle- and bar-shaped forms. The magnetococci were the most abundant, and had flagella arranged in parallel within a bundle. The majority of magnetosomes were arranged in one, two or multiple chains, although irregular arrangements were also evident. All the results of high-resolution transmission electron microscopy (HRTEM) analysis show that magnetosome crystals were composed of Fe_3O_4, and their morphology was specific to particular cell morphotypes. By the 16S rRNA gene sequence analysis, we found fourteen operational taxonomic units (OTUs) which were related to magnetotactic bacteria. Among these, thirteen belonged to the *Alphaproteobacteria* and one to the *Gammaproteobacteria*. Compared with known axenic and uncultured marine magnetotactic bacteria, the 16S rRNA gene sequences of most magnetotactic bacteria collected from the Yuehu Lake exhibited sequence identities ranging from 90.1% to 96.2% (<97%). The results indicate that microbial communities containing previously unidentified magnetotactic bacteria occur in the Yuehu Lake.

Key words: magnetotactic bacteria, magnetosome, biodiversity, Yuehu Lake, intertidal sediments

Citation: Du Haijian, Zhang Rui, Zhang Wenyan, Xu Cong, Chen Yiran, Pan Hongmiao, Zhou Ke, Wu Long-fei, Xiao Tian. 2017. Characterization of uncultivated magnetotactic bacteria from the sediments of Yuehu Lake, China. Acta Oceanologica Sinica, 36(2): 94–104, doi: 10.1007/s13131-017-0980-8

1 Introduction

Magnetotactic bacteria (MTB) are prokaryotes that can orient and swim along magnetic and geomagnetic field lines, a behavior referred to as magnetotaxis. These microorganisms were first described by Salvatore Bellini in 1963 (Bellini, 2009). In 1975, Blakemore independently rediscovered MTB, and was the first to observe magnetosomes, the organelles within cells of MTB that are responsible for their magnetotaxis (Blakemore, 1975). Magnetosomes are magnetite or greigite nanocrystals enveloped by a phospholipid bilayer membrane (Bazylinsk et al., 1995; Bazylinski and Frankel, 2004; Blakemore, 1982; Keim et al., 2003). They are usually 35–120 nm in size and are arranged in a chain configuration (Bazylinski and Moskowitz, 1997; Esquivel and De Barros, 1986; Mann et al., 1990; Stolz et al., 1989). Magnetic particles in this size range are stable single domains. The morphotypes of magnetosomes include cubo-octahedral, prisms, bullets, flakes and irregular shapes (Benzerara and Menguy, 2009; Schüler, 1999; Simmons et al., 2004). Almost all known MTB are microaerophilic, anaerobic, or facultatively anaerobic microaerophilic microbes found at the oxic-anoxic transition zone (OATZ) in sediments or chemically stratified water columns. Various groups have speculated that magnetotaxis helps MTB locate and maintain an optimal position in the vertical chemical concentration gradients that are common in stationary aquatic habitats, by reducing a three-dimensional search problem to one of a single dimension (Bazylinski and Frankel, 2004; Frankel et al., 1997).

Many morphotypes have been observed worldwide among MTB from fresh, brackish and marine waters and from soils, including coccoid to ovoid, rod, vibriod, spirillum and multicellular forms (Hanzlik et al., 2002; Lefèvre et al., 2009; Maratea and Blakemore, 1981; Sakaguchi et al., 2002; Wenter et al., 2009; Zhou et al., 2013). Under different environmental conditions the

Foundation item: The National Natural Science Foundation of China under contract Nos 41606187 and 41276170; the National Natural Science Foundation of China—Shandong Joint Fund for Marine Science Research Centers under contract No. U1406403; the National Natural Science Foundation of China under contract No. 41330962.

*Corresponding author, E-mail: txiao@qdio.ac.cn

†These authors contributed equally to this work.

factors that affect the distribution of MTB may differ (Flies et al., 2005a; Lin et al., 2014a). The adaptability of MTB to their habitats will vary depending on the species involved (Flies et al., 2005a; Lin et al., 2014a).

Studies considering about the diversity of MTB have been based on morphological characteristics and analysis of 16S rRNA gene sequences, which are considered to be the main criteria distinguishing MTB from other bacteria (Spring and Schleifer, 1995). A great diversity of MTB has been identified, with most being affiliated with two phyla: the phylum *Proteobacteria*, which includes the *Alpha*, *Gamma* and *Delta* classes; and the phylum *Nitrospirae*. Recently an uncultured magnetotactic bacterium (strain SKK-01) belonging to candidate phylum Omnitrophica was reported (Kolinko et al., 2012, 2016).

Most reported cocci, vibrios and spirilla that produce magnetite magnetosomes have been affiliated with the *Alphaproteobacteria* (Amann et al., 2006; Spring and Bazylinski, 2006). Examples of such organisms are numerous magnetococci and one magnetovibrio in Lake Chiemsee (Spring et al., 1993, 1992), two uncultured magnetococci in the Itaipu Lagoon (Brazil) (Spring et al., 1998), numerous magnetococci in the Miyun Lake and Yuandadu Park (China) (Lin et al., 2009; Lin and Pan, 2009), and magnetococci in the Huiquan Bay (China) (Pan et al., 2008; Xing et al., 2008). In addition, some cultured MTB, including marine coccoid strains MO-1 (Lefèvre et al., 2009) and *Magnetococcus marinus* strain MC-1 (Frankel et al., 1997), vibrioid strain *Magnetovibrio blakemorei* strain MV-1 (Bazylinski et al., 1988), *Magnetospira* sp. strain QH-2 (Zhu et al., 2010), freshwater magnetospirilla *Ms. Gryphiswaldense* MSR-1, *Ms. Magneticum* AMB-1, *Ms. Magnetotacticum* strain MS-1 and Magnetospirillum strain XM-1 (Arakaki et al., 2008; Balkwill et al., 1980; Bazylinski and Frankel, 2004; Matsunaga et al., 1991; Wang et al., 2015), also belong to the *Alphaproteobacteria*.

One of the most interesting magnetotactic bacteria among the *Deltaproteobacteria* are magnetotactic multicellular prokaryotes (MMPs), which are found only in saline aquatic environments but occur in large numbers (DeLong et al., 1993; Farina et al., 1990; Keim et al., 2003; Simmons et al., 2004; Wenter et al., 2009; Zhou et al., 2011, 2012, 2013). MMPs are affiliated with the order *Desulfobacterales*, and their closest (89%) phylogenetic relative is *Desulfosarcina variabilis*, a type of sulfate reducing bacterium (Abreu et al., 2007; DeLong et al., 1993; Wenter et al., 2009). In addition, two cultured rod-shaped MTB isolated from a brackish spring in the USA (Lefèvre et al., 2011c) (*Candidatus* Desulfamplus magnetomortis strain BW-1 and strain SS-2) and a rod-shaped magnetotactic bacterium (*Desulfovibrio magneticus* strain RS-1) isolated from a freshwater river in Japan (Kawaguchi et al., 1995) are also affiliated with the *Deltaproteobacteria*. Three alkaliphilic magnetotactic strains ML-1, ZZ-1 and AV-1, which were isolated from extremely alkaline environments, also belong to *Deltaproteobacteria* (Lefèvre et al., 2011b).

Magnetotactic bacteria belonging to the *Gammaproteobacteria* have also been identified. For example, a putative greigite-producing rod-shaped bacterium belonging to the *Gammaproteobacteria* was identified in a salt pond in Falmouth, Massachusetts (Simmons et al., 2004). In addition, two magnetite-producing rod-shaped bacteria, designated BW-2 and SS-5, isolated from sediment and water in California, were also found to belong to the *Gammaproteobacteria* (Lefèvre et al., 2012).

Several uncultured MTB are affiliated with the phylum *Nitrospirae*. A large rod-shaped bacterium, *Candidatus* Magnetobacterium bavaricum, was discovered in sediment samples from lakes Chiemsee and Ammersee, in southern Germany (Spring et al., 1993; Vali et al., 1987). A small rod-shaped magnetotactic member of the *Nitrospirae* was collected from sediment of the Waller Sea (Germany), and designated strain MHB-1 (Flies et al., 2005b). Two *Nitrospirae* MTB: *Candidatus* Thermomagnetovibrio paiutensis strain HSMV-1, from brackish hot springs in the USA, and *Candidatus* Magnetoovum mohavensis strain LO-1, from freshwater sediments of Lake Mead, Nevada, were described (Lefèvre et al., 2011a). A large rod-shaped MTB strain belonging to the "*Candidatus* Magnetobacterium" genus has recently been identified from the Miyun Lake near Beijing, China and its first draft genome sequence of 3.42 Mb has been assembled (Lin et al., 2014b). A kind of large magnetotactic coccus *Candidatus* Magnetoovum chiemensis strain CS-04 belonging to the deep-branching phylum *Nitrospirae* was recently identified by single-cell techniques from sediments of Lake Chiemsee (Kolinko et al., 2016). In addition, a watermelon-shaped magnetotactic organism (designated MWB-1) was found in the Beihai Lake (Beijing, China) (Lin et al., 2012).

Here we report characteristics of MTB found in the intertidal sediments of Yuehu Lake (China), including their cellular morphology, the morphology and arrangement of magnetosomes, and the features of other inclusions. The 16S rRNA gene-based approach was used to analyze the phylogenetic affiliations of the MTB found. The aim was to investigate the features of these intriguing organisms, which inhabit a shallow coastal lagoon and intertidal zone. The results reinforce the large diversity found among marine MTB, and improve understanding of the adaptation mechanisms of marine MTB to intertidal zone habitats, and their roles in biogeochemical cycles.

2 Materials and methods

2.1 *Site description*

The Yuehu Lake (36°43′–37°27′N, 122°09′–122°42′E; approximately 4.94 km^2; also known as the Swan Lake) is a shallow coastal lagoon located on the east side of Shandong Peninsula, China (Fig. 1a). The pH value of lake water changes from 7.9 to 8.5, and the salinity varies at the range of 29.6–34.1. It is encircled by land to the north, west and south, and is connected to the Rongcheng Bay in the Yellow Sea by an entrance channel (approximately 85 m) to the southeast, forming a relative stable lagoon-tidal inlet system (Fig. 1a). There are several seasonal rivulets flowing into the lake, and there is a large area of reed swamp in the northern and western wetland. A large number of swans overwinter in the area each year. The environmental conditions in the lake have deteriorated in recent years as a result of excessive nutrient inputs and intensification of aquaculture of shrimp and sea cucumber. In spring, large quantities of marine plants, including eelgrass, bloom in the lake. The swans, aquaculture, freshwater inputs and human activities lead to increased organic matter and organisms in the sediments of this lake (Gao et al., 2013).

2.2 *Sampling and collection of MTB*

The sampling site (37°21′33.857″N, 122°34′41.571″E) was in the mid tidal region of the intertidal zone in the northern part of Yuehu Lake, where a rivulet enters the lake (Fig. 1b).

During the period of September to October 2013, sediment samples were collected on three occasions at approximately two-week intervals during ebb tides. The sediments were yellow and sandy at the surface, whereas the subsurface layers were gray-black (Fig. 1c). Subsurface sediments and seawater (~1:1) were collected and stored in 500-mL plastic bottles. Cells were en-

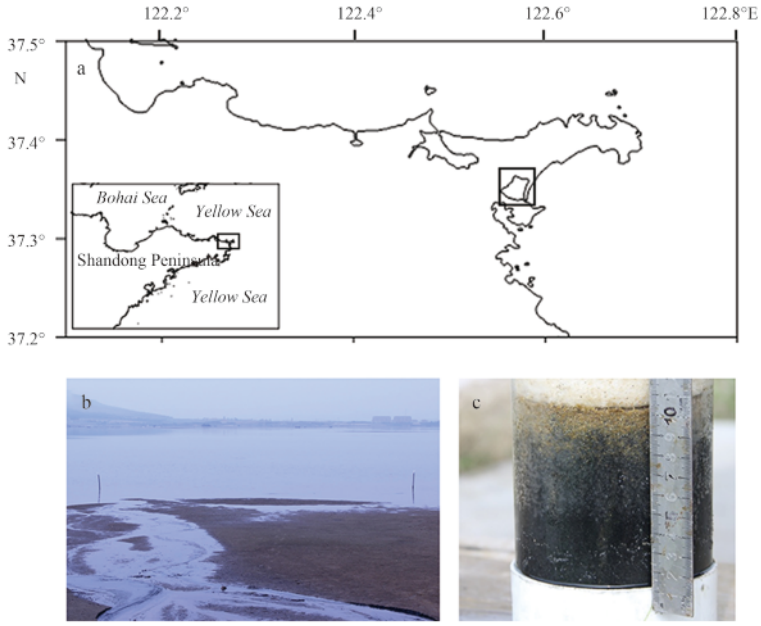

Fig. 1. Location of the sampling site. a. Map of Shandong Peninsula showing the location of Yuehu Lake (black frame), b. the Yuehu Lake sampling site, and c. the distribution of the sandy layer in the Yuehu Lake.

riched by attaching the south pole of a permanent magnet (0.05 T) outside the bottle and 1 cm above the sediment surface. After 30 to 40 min, the water near the south pole of the magnet was collected using a pipette and transferred to a 1.5 mL tube (volumes were recorded as V_1 mL). For transmission electron microscopy (TEM) and analysis of 16S rRNA gene sequences, the enriched MTB were purified using the race track method (Jogler et al., 2009; Lins et al., 2003; Wolfe et al., 1987).

2.3 *Optical and electron microscopy*

A 30 μL (V_2/mL) sample of each concentrate was used to prepare a hanging drop (Schüler, 2002) for microscopic examination. The numbers of unicellular MTB were counted as n (ind.), and the dominant morphotype of unicellular MTB was determined using optical microscopy (Olympus BX51, equipped with a DP71 camera system; Olympus, Tokyo, Japan).

The abundance of MTB (N, ind./cm^3) was calculated using the formula $N = nV_1/V_2V$, where V (cm^3) is the volume of sediment in each bottle. The abundance of MTB was calculated from 150 samples.

For TEM a 3–5 μL volume of purified sample was deposited on a Formvar-coated copper grid (Emcn, Beijing, China) for 3–5 min; the grid was then washed with distilled water and air dried.

Samples for fluorescence microscopy were fixed in glutaraldehyde (final concentration 1.25%) for 15 min, washed with sterile distilled water, and stained with 4′, 6′-diamidino-2-phenylindole (DAPI) for 15 min. The stained cells were washed with distilled water, and observed using a fluorescence microscope equipped with a mercury arc UV/visible light source (Olympus, Tokyo, Japan).

Samples for observations of flagella were stained with 1% uranyl acetate for 1 min. The morphology and structure of the MTB were analyzed using a Hitachi H8100 TEM operated at 75 kV. The crystal structures and chemical compositions of the magnetosomes were analyzed by high-resolution transmission electron microscopy (HRTEM) using a JEM2100 transmission electron microscope operated at 200 kV and equipped for energy dispersive X-ray spectroscopy (EDXS).

The length and width of magnetosomes were measured using images imported into Adobe Photoshop. The size and shape factors for the magnetosomes were calculated as (length+width)/2 and width/length, respectively (Lin and Pan, 2009).

2.4 *Sequence analysis of the 16S rRNA gene*

The purified magnet-enriched MTB were washed three times with sterile distilled water. The samples were freeze-thawed three times by freezing in liquid nitrogen and thawing at 100°C. Amplification of the 16S rRNA gene was achieved by PCR in an Eppendorf Mastercycler, using the universal bacterial primers 27F (5′-AGAGTTTGATCCTGGCTCAG-3′) and 1492R (5′-GGTTACCTTGTTACGACTT-3′) (Sangon Biotech, Shanghai, China). The PCR products were purified, cloned into pMD18-T vectors (Takara, Dalian, China), and transformed into competent *E. scherichia* coli Top10 cells (Tiangen Biotech, Beijing, China). The clones were sequenced using the specific primers RV-M and M-13 (Sangon Biotech, Shanghai, China).

The sequences obtained were analyzed using the BLAST program (http://www.ncbi.nlm.nih.gov/BLAST/) (Altschul et al., 1997), and the available 16S rRNA gene sequences of MMPs were obtained from the GenBank database. Alignment of all 16S rRNA genes was performed using the CLUSTAL W multiple alignment program (Thompson et al., 1994). Identity was calculated using BIOEDIT software, and the phylogenetic tree was constructed using the neighbor-joining method, as applied in MEGA Version 4 (Kumar et al., 2008; Tamura et al., 2007). Bootstrap values were calculated from 1 000 replicates.

The Jaccard index (J) was calculated to evaluate the similarity of MTB communities in the intertidal sediments of Yuehu Lake (Xing et al., 2008) and Taiping Bay, Qingdao (Xu et al., 2016) as follows:

$$J = \frac{|A \cap B|}{|A \cup B|},$$

where $|A \cap B|$ refer to the number of OTUs which are the same (>

97%) from Site A and Site B, $|A \cup B|$ refer to the number of all the OTUs that obtained from Site A and Site B.

3 Results

3.1 *Morphology of magnetotactic bacteria*

Based on TEM, diverse morphotypes of unicellular MTB were present in the intertidal sediments of Yuehu Lake. More than 90% of those observed were cocci or oval-shaped, with an average size of (1.78±0.48)×(1.42±0.39) μm (n=54) (Figs 2a–f). The second most abundant type was vibrio cells, which had an average size of (2.93±1.31)×(0.95±0.65) μm (n=10) (Figs 2g–i). Other morphotypes including rod-shaped (Figs 2j, k and n), handle-shaped (Fig. 2l) and spirilla (Fig. 2m) were also observed. In particular, a large (7.69×1.63 μm) rod-shaped MTB was observed (Fig. 2n).

Based on optical microscopy, the abundance of MTB reached 10^3–10^4 ind./cm^3; these were dominated by magnetococci (> 90%), but lesser numbers of vibrios and spirilla were also present. Approximately 95% of the MTB displayed north-seeking taxis in the presence of an applied magnetic field (Fig. 3). Our TEM analysis allowed us to observe flagella for cocci and oval-shaped MTB. Flagella in these morphotypes were arranged in parallel within a bundle. The length of the flagella was a factor of 1–2 longer than the length (diameter) of the cell, and the diameter was 70.8±14.6 nm. Some of the magnetococci had a single flagellar bundle, while others had two or three bundles on the same side of the cell (Fig. 3, Fig. A1).

3.2 *Magnetosomes*

Using TEM, diverse arrangements of magnetosomes were observed. The arrangement of magnetosomes in the magnetococci that dominated among MTB is shown in Fig. 2. Most magnetococci had two magnetosome chains arranged in parallel (Fig. 2d) or crossing (Fig. 2a). A minority had only one magnetosome chain (Fig. 2c). Magnetosomes arranged in a cluster (Fig. 2b) or in multiple parallel chains (Fig. 2e) were also observed. MTB hav-

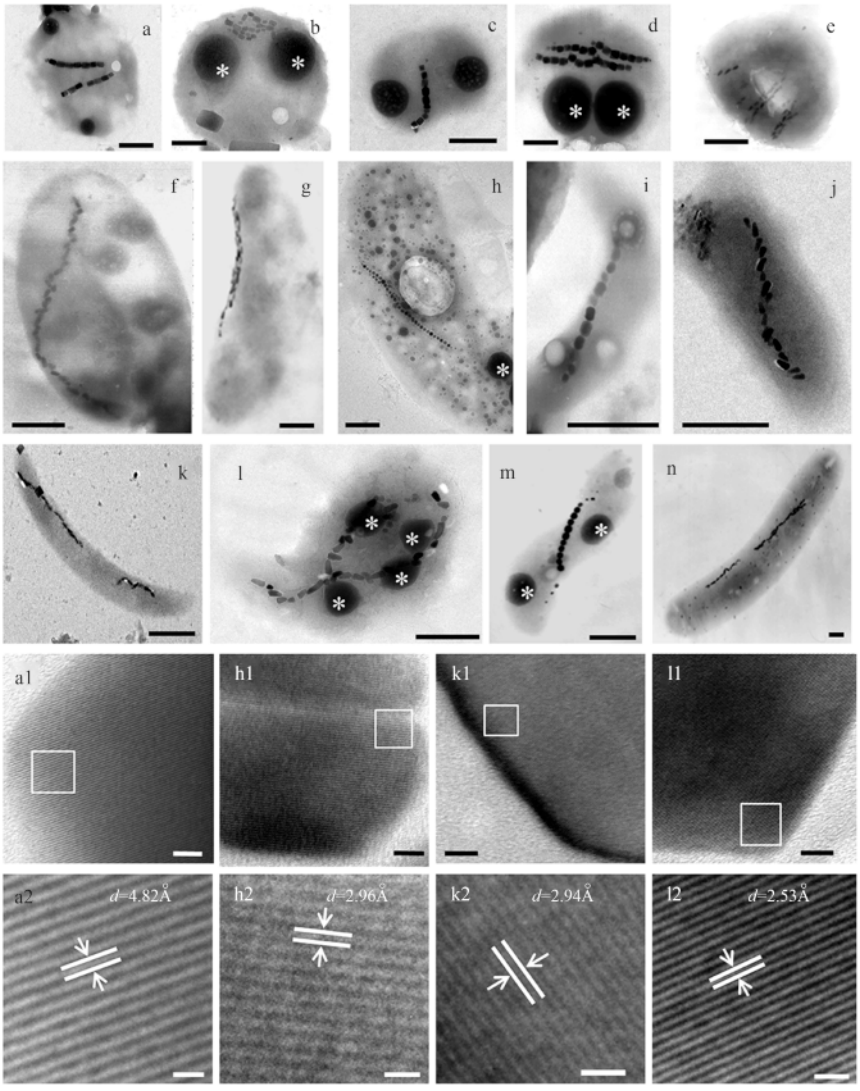

Fig. 2. TEM micrographs of individual cells and magnetosomes of marine MTB collected from the Yuehu Lake. a, b, c, d and e. Coccoid; f. oval-shaped; g, h and i. vibriod; j, k and n. rod-shaped; l. handle-shaped; and m. spirillum. * indicate dense black granules in the cells. Scale bars is 500 nm. a1, h1, k1 and l1 are HRTEM analysis of prismatic, cubo-octahedral, bullet-shaped and tooth-(or flake-) shaped magnetosomes in a, h, k, l, respectively. Scale bars is 5 nm. a2, h2, k2 and l2 are the magnification of a selected area in a1, h1, k1, l1, respectively. Scale bars are 1 nm.

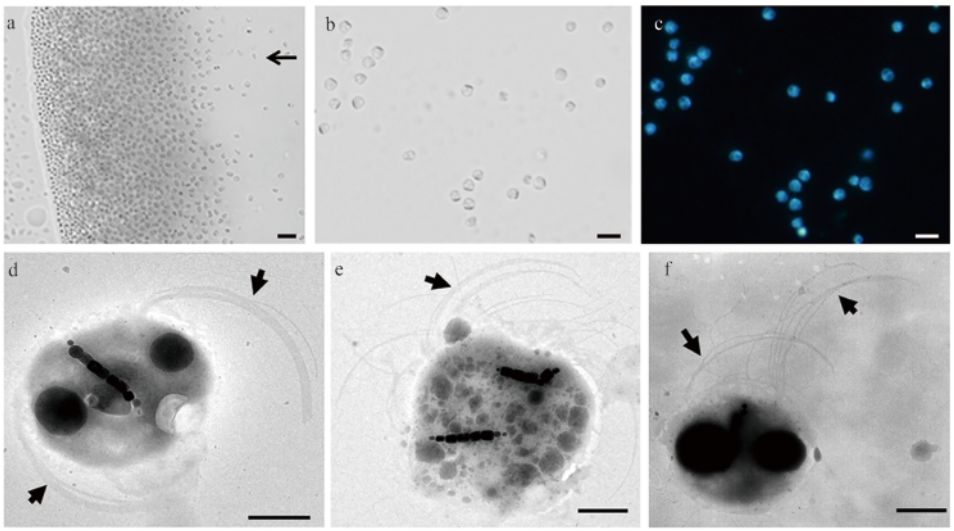

Fig. 3. Morphology and the flagella of marine magnetococci. a. MTB gathered at the edge of a water drop under the influence of an applied magnetic field (95% were north-seeking MTB) (The black arrow indicates the direction of the magnetic field lines), b. differential interference contrast (DIC) image of magnetococci, c. DAPI stained cells showing the morphology of magnetococci, and d–f. TEM micrographs showing the MTB cell has two bundles of flagella (black arrows). Scale bars are 5 m in Panels a–c and 500 nm in the other panels.

ing spirillum (Fig. 2m), vibrio (Figs 2g–i) and rod (Figs 2j, k and n) morphologies had one or multiple magnetosome chains aligned along the long axis of the cell, although the magnetosome morphotypes, sizes and quantities differed. Magnetosomes aligned in a circled chain were observed in handle-shaped MTB (Fig. 2l).

Four main types of magnetosomes were observed (Table 1, Fig. A2). In some degree, the shape and morphology of the magnetosome crystals were specific to particular cell morphotypes, and included prismatic magnetosomes in magnetococci (Figs 2a–d), vibrio (Fig. 2i, Fig. A3b) and spirillum cells (Fig. 2m), bullet-shaped magnetosomes in magnetococci (Figs 2e and f), rods (Figs 2j, k and n) and vibrio cells (Fig. 2g), tooth- or flake-shaped magnetosomes in handle-shaped MTB (Fig. 2l), and cubo-octahedral magnetosomes in vibrio cells (Fig. 2h). All the results of EDXS analysis indicated that magnetosome crystals were composed of iron and oxygen (Figs A4a–d). This was consistent with the results of HRTEM analysis, which identified the magnetosome crystals as magnetite (Fe_3O_4) (Table 1; Figs 2a1, h1, k1, l1, a2, h2, k1, and l2).

Table 1. Characteristics of the four types of magnetosome

Morphology of magnetosomes	Size/nm	Mean size/nm	Breadth-length ratio	Composition	*n*
Prism-shaped (in magnetococci)	(97.7±24.8)×(80.9±24.0)	80.9±24.0	0.83±0.11	Fe_3O_4	198
Cubo-octahedral	(53.1±5.9)×(50.2±5.6)	51.6±5.6	0.94±0.04	Fe_3O_4	32
Bullet-shaped	(97.6±28.4)× (42.6±7.2)	70.1±17.0	0.46±0.09	Fe_3O_4	61
Tooth- or flake-shaped	(90.3±30.2)×(54.2±6.0)	72.2±16.8	0.65±0.17	Fe_3O_4	41

The MTB also contained several (1–4) phosphorus granules (Figs 2d and l). EDXS analysis revealed that the granules were rich in phosphorus and oxygen (Figs A4e and f); these may be polyphosphate, as reported for other MTB (Cox et al., 2002; Keim et al., 2001, 2005; Lefèvre et al., 2009; Lins and Farina, 1999; Silva et al., 2008). Phosphorus granules are considered to be involved in the accumulation of phosphates, metal ions and organic compounds (Lins and Farina, 1999). Whether these granules are involved in the accumulation of iron or the formation of magnetosomes remains to be determined.

3.3 *Diversity analysis based on 16S rRNA gene clone libraries*

Phylogenetic analysis based on 16S rRNA gene sequences was performed to investigate the structure of the MTB community. A total of 88 positive clones were obtained, 29 of which contained sequences indicative of MTB. These 29 sequences were composed of 14 operational taxonomic units (OTUs), which were defined at the 97% similarity level. The 14 OTUs have been submitted to GenBank as MRC-2 (KJ591588), MRC-5 (KJ591589), MRC-12 (KJ591590), MRC-13 (KJ591591), MRC-14 (KJ591592), MRC-19 (KJ591593), MRC-29 (KJ591594), MRC-66 (KJ591598), MRC-71 (KJ591601), MRC-83 (KJ591599), MRC-93 (KJ591600), MRC-106 (KJ591595), MRC-110 (KJ591596) and MRC-112 (KJ591597).

Phylogenetic analysis demonstrated that MRC-13 is 93.9% identical to the cultured MTB BW-2 (HQ595728), and belongs to the *Gammaproteobacteria*. The other OTUs were all found to belong to the *Alphaproteobacteria*. MRC-2 was 96.2% identical to MC-1 (CP000471); MRC-12 was 93.6% identical to the uncultured marine magnetococcus M-67 (EF371491); MRC-106 was 90.1% identical to clone 1–3 (JF421219); MRC-93, MRC-71, MRC-66, MRC-29 and MRC-14 were 92.9%, 93.0%, 95.4%, 95.5% and 97.2% identical to the uncultured marine magnetococcus MRT-130 (from the Huiquan Bay, Qingdao), respectively; MRC-110 and MRC-112 were 92.0% and 97.5% identical to MRT-122, respectively; MRC-19 was 95.6% identical to MRT-134; and MRC-5

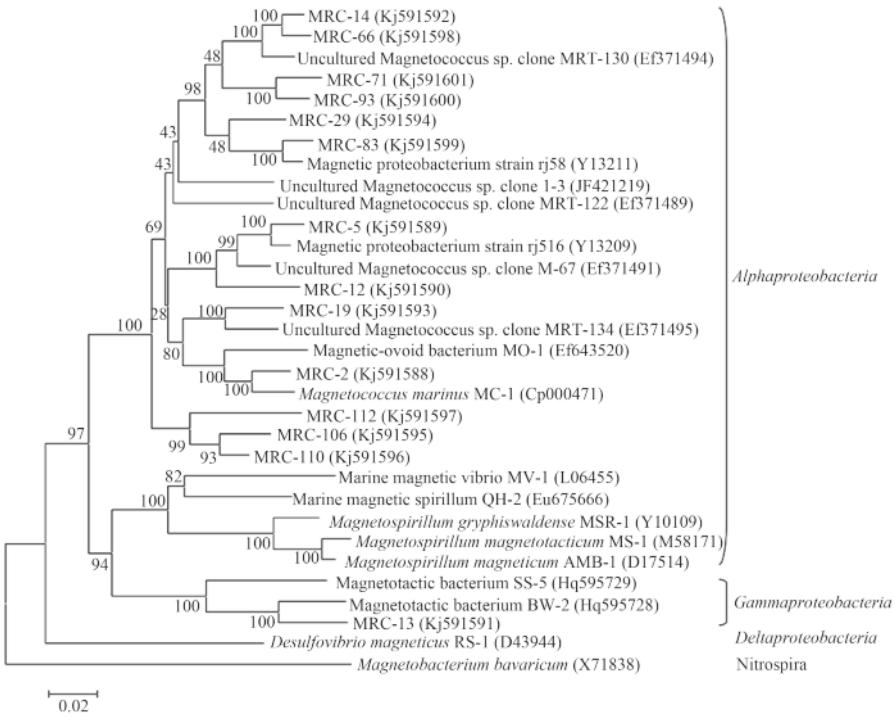

Fig. 4. Phylogenetic tree showing the relationship between potential marine MTB from the Yuehu Lake and related MTB.

and MRC-83 were 97.6% identical to strains rj516 (Y13209) and rj58 (Y13211), respectively (Fig. 4).

The sequence determined in this study is shown in bold. The GenBank accession numbers of the sequences used are indicated in parentheses. Scale bar is 0.02 substitutions per nucleotide position.

Among the 14 OTUs, MRC-71 was 96.5% identical to MRC-93, MRC-106 was 96.1% identical to MRC-110, MRC-14 was 94.7% identical to MRC-29, MRC-29 was 94.5% identical to MRC-83, and MRC-14 was 94.4% identical to MRC-66. The similarities among the other OTUs were all less than 93%.

Comparison among the OTUs obtained from MTB communities of the intertidal zone of Taiping Bay and the subtidal zone of Huiquan Bay suggests that the MTB community in the sediment of Yuehu Lake is most similar to that in the Taiping Bay (Jaccard index is 0.1250) (Xu et al., 2016), and less similar to that in the Huiquan Bay (Jaccard index is 0.047 6) (Fig. 5) (Xing et al., 2008).

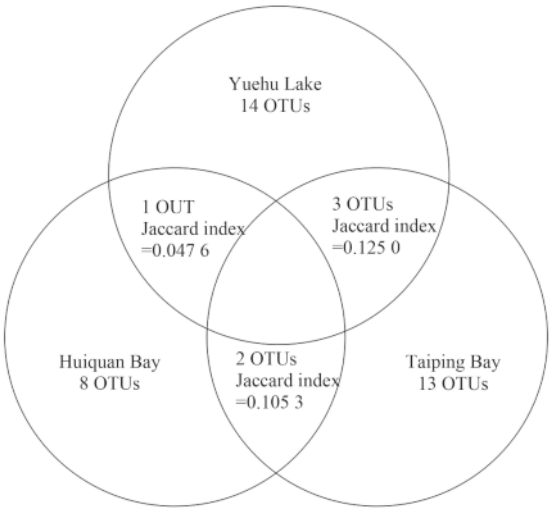

Fig. 5. Comparison of magnetotactic bacteria communites from the intertidal sediments of Yuehu Lake, Huiquan Bay and Taiping Bay in Qingdao.

4 Discussion

The concentration of MTB in the intertidal sediments of Yuehu Lake was found to be 10^3–10^4 ind./cm^3, which is similar to the levels reported previously for general environments from which these bacteria have been found (Blakemore, 1982). However, it is lower than the concentration reported for the Huiquan Bay (Xing et al., 2008) (10^5 ind./cm^3) and for some freshwater samples (Flies et al., 2005a) (10^7 ind./cm^3), but higher than that in the intertidal sediments of Taiping Bay (350 ind./cm^3) (Xu et al., 2016).

Most previously reported morphotypes of MTB were found in the sediment samples collected from the Yuehu Lake. Magnetococci were the dominant form (> 90%) observed in the Yuehu Lake, consistent with previously reported MTB morphotypes (Flies et al., 2005b; Lin et al., 2009; Lin and Pan, 2009; Pan et al., 2008; Spring et al., 1993, 1998). The magnetococci had flagella arranged in parallel within a bundle, which may be similar to other MTB from marine environments like MO-1 or MC-1 (Lefèvre et al., 2009).

The magnetosomes were all found to be composed of Fe_3O_4 and the morphology of the magnetosome crystals was specific to particular cell morphotypes, consistent with previous findings (Meldrum et al., 1993). For example, prismatic magnetosomes were found in magnetococci, vibrio and spirillum cells, bullet-shaped magnetosomes were observed in magnetococci, rod-shaped or vibrio MTB, cubo-octahedral magnetosomes were found in vibrio cells, and tooth- or flake-shaped magnetosomes were found in handle-shaped MTB. In the MTB collected in the Yuehu Lake, the dominant magnetosome morphology was pris-

matic. The majority of magnetosomes were arranged in one, two or multiple chains. The arrangement of magnetosome in MTB may be a reflection of genetic diversity. It is intriguing and needs more research.

The 16S rRNA gene sequence analysis suggested the presence of at least 14 taxonomic groups which are related to MTB. The results indicate that considerable resource of MTB species occur in the Yuehu Lake. The MTB community in the sediment of Yuehu Lake is most similar to that in the Taiping Bay and less similar to that in the Huiquan Bay by comparison. These differences may be due to differences in habitat characteristics. The sampling site in the Huiquan Bay is influenced by human activities, particularly a nearby bathing beach. It is possible that MTB are sensitive to external factors affecting their habitat, influencing the presence or absence of some MTB species. The Yuehu Lake is a relative stable lagoon-tidal inlet system, and thus differs from the Huiquan Bay, which has an environment that changes dramatically. The difference in the MTB communities at these locations may reflect differences in their adaptability, with some MTB species preferring a stable environment. However, the abundance of MTB was greater in the Huiquan Bay. This may be because of the presence of freshwater input near the sampling site, which introduces organic matter to the MTB habitat.

Among the 88 positive clones, MRC-14 and MRC-71 both had eight sequences (9.0%), showing that they were both the most dominant species in MTB. Two sequences belong to MRC-2, and the other OTUs had only one, respectively. Among the OTUs obtained from MTB communities of the intertidal zone of Taiping Bay (Xu et al., 2016), the most abundant one is XCQD1-18 (KM083474), which is 98.6% identical to MRC-14, suggesting that this kind of organism may be the most dominant species under the environment like the intertidal zone of Yuehu Lake or Taiping Bay.

So far bullet-shaped magnetosomes have been mainly identified in the MTB belonging to *Deltaproteobacteria*, the phylum *Nitrospirae* and candidate phylum Omnitrophica (Lefèvre and Wu, 2013). However, no sequences are related to *Deltaproteobacteria* and phylum *Nitrospirae* in our results. Actually, most of MTB (> 90%) that we observed were magnetococci with prism-shaped magnetosomes. The large number may lead to the result that MTB belonging to *Alphaproteobacteria* were inclined to be detected by 16S rRNA gene sequence analysis. The proportions of *Deltaproteobacteria* and phylum *Nitrospirae* may be too small to be detected by this analysis.

We have previously reported the presence of MMPs from the same location as in this study (Chen et al., 2015; Zhang et al., 2014). Characterization and phylogenetic identification indicated the presence of only one species of spherical MMP (*Candidatus* Magnetomorum rongchengroseum) and only one ellipsoidal MMP species (*Candidatus* Magnetananas rongchenensis), both of which are monospecific. Previous studies have also shown that MMPs from the Yuehu Lake can produce bullet-shaped magnetite magnetosomes and equidimensional greigite magnetosomes. The unicellular MTB were found to be different from the MMPs in many aspects. The unicellular MTB from the Yuehu Lake comprise many species showing diverse cellular and magnetosome morphologies. However, the magnetosomes of the unicellular MTB were composed of magnetite, and no greigite magnetosomes were found. This difference may be related to the different habitats of the unicellular MTB and the MMPs. Our results suggest that most of the unicellular MTB were distributed in the surface layer of sediment, while the MMPs occur at greater depth (approximately 2–6 cm) (unpublished data), where the environment is more reducing and the concentration of reduced sulfur is higher. We only found ellipsoidal MMPs containing greigite magnetosomes in autumn, when the highest concentrations of total sulfur occurred. It is possible that the MMPs produce greigite magnetosomes in response to an increase in the reduced sulfur concentration (Bazylinsk et al., 1995; Lefèvre et al., 2011c). In contrast, the unicellular MTB were always found in oxidizing environments lacking reduced sulfur, which may explain why they produce only magnetite magnetosomes.

The phylogenetic diversity of magnetotactic bacteria in axenic culture or collected from natural environments is currently primarily based on 16S rRNA gene sequence analysis, or phenotypic characteristics including cell morphology and features of the magnetosomes. In this study we did not confirm whether the morphology of the magnetosome crystals corresponds to the phylogenetic position of the MTB. To assess the relationship between these two aspects, further research will be needed on the gene(s) affecting the formation of magnetosome crystals and chains.

Acknowledgements

This study was supported by Laboratoire International Associé de la Bio-Minéralisation et Nano-Structures. We thank Xu Jianhong and Zheng Xin for kind assistance in sampling, Jiang Ming and Ma Xicheng for help with TEM observations.

References

Abreu F, Martins J L, Silveira T S, et al. 2007. '*Candidatus* magnetoglobus multicellularis', a multicellular, magnetotactic prokaryote from a hypersaline environment. Int J Syst Evol Microbiol, 57(6): 1318–1322

Altschul S F, Madden T L, Schäffer A A, et al. 1997. Gapped BLAST and PSI-BLAST: a new generation of protein database search programs. Nucleic Acids Res, 25(17): 3389–3402

Amann R, Peplies J, Schüler D. 2006. Diversity and taxonomy of magnetotactic bacteria. In: Schüler D, ed. Magnetoreception and Magnetosomes in Bacteria: Microbiology Monographs. Berlin Heidelberg: Springer, 25–36

Arakaki A, Nakazawa H, Nemoto M, et al. 2008. Formation of magnetite by bacteria and its application. J Roy Soc Interface, 5(26): 977–999

Balkwill D L, Maratea D, Blakemore R P. 1980. Ultrastructure of a magnetotactic spirillum. J Bacteriol, 141(3): 1399–1408

Bazylinski D A, Frankel R B. 2004. Magnetosome formation in prokaryotes. Nat Rev Microbiol, 2(3): 217–230

Bazylinski D A, Frankel R B, Heywood B R, et al. 1995. Controlled biomineralization of magnetite (Fe_3O_4) and greigite (Fe_3S_4) in a magnetotactic bacterium. Appl Environ Microbiol, 61(9): 3232–3239

Bazylinski D A, Frankel R B, Jannasch H W. 1988. Anaerobic magnetite production by a marine, magnetotactic bacterium. Nature, 334(6182): 518–519

Bazylinski D A, Moskowitz B M. 1997. Microbial biomineralization of magnetic iron minerals: microbiology, magnetism and environmental significance. Rev Miner Geochem, 35(1): 181–223

Bellini S. 2009. On a unique behavior of freshwater bacteria. Chin J Oceanol Limnol, 27(1): 3–5

Benzerara K, Menguy N. 2009. Looking for traces of life in minerals. Cr Palevol, 8(7): 617–628

Blakemore R P. 1975. Magnetotactic bacteria. Science, 190(4212): 377–379

Blakemore R P. 1982. Magnetotactic bacteria. Annu Rev Microbiol, 36(1): 217–238

Chen Yiran, Zhang Rui, Du Haijian, et al. 2015. A novel species of ellipsoidal multicellular magnetotactic prokaryotes from Lake Yuehu in China. Environ Microbiol, 17(3): 637–647

Cox B L, Popa R, Bazylinski D A, et al. 2002. Organization and elemental analysis of P-, S-, and Fe-rich inclusions in a population of freshwater magnetococci. Geomicrobiol J, 19(4): 387–406

DeLong E F, Frankel R B, Bazylinski D A. 1993. Multiple evolutionary origins of magnetotaxis in bacteria. Science, 259(5096): 803–806

Esquivel D M S, De Barros H G P. 1986. Motion of magnetotactic microorganisms. J Exp Biol, 121(1): 153–163

Farina M, Esquivel D M S, De Barros H G P L. 1990. Magnetic iron-sulphur crystals from a magnetotactic microorganism. Nature, 343(6255): 256–258

Flies C B, Jonkers H M, de Beer D, et al. 2005a. Diversity and vertical distribution of magnetotactic bacteria along chemical gradients in freshwater microcosms. FEMS Microbiol Ecol, 52(2): 185–195

Flies C B, Peplies J, Schüler D. 2005b. Combined approach for characterization of uncultivated magnetotactic bacteria from various aquatic environments. Appl Environ Microbiol, 71(5): 2723–2731

Frankel R B, Bazylinski D A, Johnson M S, et al. 1997. Magneto-aerotaxis in marine coccoid bacteria. Biophys J, 73(2): 994–1000

Gao Li, Zhang Luhua, Hou Jinzhi, et al. 2013. Decomposition of macroalgal blooms influences phosphorus release from the sediments and implications for coastal restoration in Swan Lake, Shandong, China. Ecol Eng, 60: 19–28

Hanzlik M, Winklhofer M, Petersen N. 2002. Pulsed-field-remanence measurements on individual magnetotactic bacteria. J Magn Magn Mater, 248(2): 258–267

Jogler C, Lin Wei, Meyerdierks A, et al. 2009. Toward cloning of the magnetotactic metagenome: identification of magnetosome island gene clusters in uncultivated magnetotactic bacteria from different aquatic sediments. Appl Environ Microbiol, 75(12): 3972–3979

Kawaguchi R, Burgess J G, Sakaguchi T, et al. 1995. Phylogenetic analysis of a novel sulfate-reducing magnetic bacterium, RS-1, demonstrates its membership of the δ-Proteobacteria. FEMS Microbiol Lett, 126(3): 277–282

Keim C N, Lins U, Farina M. 2001. Elemental analysis of uncultured magnetotactic bacteria exposed to heavy metals. Can J Microbiol, 47(12): 1132–1136

Keim C N, Lins U, Farina M. 2003. Iron oxide and iron sulphide crystals in magnetotactic multicellular aggregates. Acta Microsc, 12: 3–4

Keim C N, Solórzano G, Farina M, et al. 2005. Intracellular inclusions of uncultured magnetotactic bacteria. Int Microbiol, 8(2): 111–117

Kolinko S, Jogler C, Katzmann E, et al. 2012. Single-cell analysis reveals a novel uncultivated magnetotactic bacterium within the candidate division OP3. Environ Microbiol, 14(7): 1709–1721

Kolinko S, Richter M, Glöckner F O, et al. 2016. Single-cell genomics of uncultivated deep-branching magnetotactic bacteria reveals a conserved set of magnetosome genes. Environ Microbiol, 18(1): 21–37

Kumar S, Nei M, Dudley J, et al. 2008. MEGA: A biologist-centric software for evolutionary analysis of DNA and protein sequences. Brief Bioinform, 9(4): 299–306

Lefèvre C T, Bernadac A, Yuzhang K, et al. 2009. Isolation and characterization of a magnetotactic bacterial culture from the Mediterranean Sea. Environ Microbiol, 11(7): 1646–1657

Lefèvre C T, Frankel R B, Abreu F, et al. 2011a. Culture-independent characterization of a novel, uncultivated magnetotactic member of the *Nitrospirae* phylum. Environ Microbiol, 13(2): 538–549

Lefèvre C T, Frankel R B, Pósfai M, et al. 2011b. Isolation of obligately alkaliphilic magnetotactic bacteria from extremely alkaline environments. Environ Microbiol, 13(8): 2342–2350

Lefèvre C T, Menguy N, Abreu F, et al. 2011c. A cultured greigite-producing magnetotactic bacterium in a novel group of sulfate-reducing bacteria. Science, 334(6063): 1720–1723

Lefèvre C T, Viloria N, Schmidt M L, et al. 2012. Novel magnetite-producing magnetotactic bacteria belonging to the *Gammaproteobacteria*. ISME J, 6(2): 440–450

Lefèvre C T, Wu Longfei. 2013. Evolution of the bacterial organelle responsible for magnetotaxis. Trends Microbiol, 21(10): 534–543

Lin Wei, Bazylinski D A, Xiao Tian, et al. 2014a. Life with compass: diversity and biogeography of magnetotactic bacteria. Environ Microbiol, 16(9): 2646–2658

Lin Wei, Deng Aihua, Wang Zhang, et al. 2014b. Genomic insights into the uncultured genus '*Candidatus* Magnetobacterium' in the phylum *Nitrospirae*. ISME J, 8(12): 2463–2477

Lin Wei, Li Jinhua, Pan Yongxin. 2012. Newly isolated but uncultivated magnetotactic bacterium of the phylum *Nitrospirae* from Beijing, China. Appl Environ Microbiol, 78(3): 668–675

Lin Wei, Li Jinhua, Schüler D, et al. 2009. Diversity analysis of magnetotactic bacteria in Lake Miyun, northern China, by restriction fragment length polymorphism. Syst Appl Microbiol, 32(5): 342–350

Lin Wei, Pan Yongxin. 2009. Uncultivated magnetotactic cocci from Yuandadu Park in Beijing, China. Appl Environ Microbiol, 75(12): 4046–4052

Lins U, Farina M. 1999. Phosphorus-rich granules in uncultured magnetotactic bacteria. FEMS Microbiol Lett, 172(1): 23–28

Lins U, Freitas F, Keim C N, et al. 2003. Simple homemade apparatus for harvesting uncultured magnetotactic microorganisms. Braz J Microbiol, 34(2): 111–116

Mann S, Sparks N H C, Board R G. 1990. Magnetotactic bacteria: microbiology, biomineralization, palaeomagnetism and biotechnology. Adv Microb Physiol, 31: 125–181

Maratea D, Blakemore R P. 1981. *Aquaspirillum magnetotacticum* sp. nov., a Magnetic Spirillum. Int J Syst Bacteriol, 31(4): 452–455

Matsunaga T, Sakaguchi T, Tadokoro F. 1991. Magnetite formation by a magnetic bacterium capable of growing aerobically. Appl Microbiol Biotechnol, 35(5): 651–655

Meldrum F C, Mann S, Heywood B R, et al. 1993. Electron microscopy study of magnetosomes in a cultured coccoid magnetotactic bacterium. Proc Roy Soc B Biol Sci, 251(1332): 231–236

Pan Hongmiao, Zhu Kailing, Song Tao, et al. 2008. Characterization of a homogeneous taxonomic group of marine magnetotactic cocci within a low tide zone in the China Sea. Environ Microbiol, 10(5): 1158–1164

Sakaguchi T, Arakaki A, Matsunaga T. 2002. *Desulfovibrio magneticus* sp. nov., a novel sulfate-reducing bacterium that produces intracellular single-domain-sized magnetite particles. Int J Syst Evol Microbiol, 52(1): 215–221

Schüler D. 1999. Formation of magnetosomes in magnetotactic bacteria. J Mol Microbiol Biotechnol, 1(1): 79–86

Schüler D. 2002. The biomineralization of magnetosomes in *Magnetospirillum gryphiswaldense*. Int Microbiol, 5(4): 209–214

Silva K T, Abreu F, Keim C N, et al. 2008. Ultrastructure and cytochemistry of lipid granules in the many-celled magnetotactic prokaryote, '*Candidatus* Magnetoglobus multicellularis'. Micron, 39(8): 1387–1392

Simmons S L, Sievert S M, Frankel R B, et al. 2004. Spatiotemporal distribution of marine magnetotactic bacteria in a seasonally stratified coastal salt pond. Appl Environ Microbiol, 70(10): 6230–6239

Spring S, Amann R, Ludwig W, et al. 1992. Phylogenetic diversity and identification of nonculturable magnetotactic bacteria. Syst Appl Microbiol, 15(1): 116–122

Spring S, Amann R, Ludwig W, et al. 1993. Dominating role of an unusual magnetotactic bacterium in the microaerobic zone of a freshwater sediment. Appl Environ Microbiol, 59(8): 2397–2403

Spring S, Bazylinski D A. 2006. Magnetotactic bacteria. In: Dworkin M, Falkow S, Rosenberg E, et al., eds. The Prokaryotes. New York: Springer, 2: 842–862

Spring S, Lins U, Amann R, et al. 1998. Phylogenetic affiliation and ultrastructure of uncultured magnetic bacteria with unusually large magnetosomes. Arch Microbiol, 169(2): 136–147

Spring S, Schleifer K H. 1995. Diversity of magnetotactic bacteria. Syst Appl Microbiol, 18(2): 147–153

Stolz J F, Chang S B R, Kirschvink J L. 1989. Biogenic magnetite in

stromatolites: I. Occurrence in modern sedimentary environments. Precambrian Res, 43(4): 295–304

Tamura K, Dudley J, Nei M, et al. 2007. MEGA4: molecular evolutionary genetics analysis (MEGA) software version 4.0. Mol Biol Evol, 24(8): 1596–1599

Thompson J D, Higgins D G, Gibson T J. 1994. CLUSTAL W: improving the sensitivity of progressive multiple sequence alignment through sequence weighting, position-specific gap penalties and weight matrix choice. Nucleic Acids Res, 22(22): 4673–4680

Vali H, Forster O, Amarantidis G, et al. 1987. Magnetotactic bacteria and their magnetofossils in sediments. Earth and Planetary Science Letters, 86(2–4): 389–400

Wang Yinzhao, Lin Wei, Li Jinhua, et al. 2015. Characterizing and optimizing magnetosome production of *Magnetospirillum* sp. XM-1 isolated from Xi'an City Moat, China. FEMS Microbiol Lett, 362(21): 1–8, doi: 10.1093/femsle/fnv167

Wenter R, Wanner G, Schüler D, et al. 2009. Ultrastructure, tactic behaviour and potential for sulfate reduction of a novel multicellular magnetotactic prokaryote from North Sea sediments. Environ Microbiol, 11(6): 1493–1505

Wolfe R S, Thauer R K, Pfennig N. 1987. A 'capillary racetrack' method for isolation of magnetotactic bacteria. FEMS Microbiol Lett, 45(1): 31–35

Xing Su'e, Pan Hongmiao, Zhu Kailing, et al. 2008. Diversity of marine magnetotactic bacteria in the Huiquan bay near Qingdao city. High Technol Lett (in Chinese), 18(3): 312–317

Xu Cong, Zhang Wenyan, Chen Yiran, et al. 2016. Diversity of magnetotactic bacteria in the intertidal zone of Taiping Bay, Qingdao. Acta Ecol Sinica, 36(14): 4346–4354, doi: 10.5846/stxb201412012380

Zhang Rui, Chen Yiran, Du Haijian, et al. 2014. Characterization and phylogenetic identification of a species of spherical multicellular magnetotactic prokaryotes that produces both magnetite and greigite crystals. Res Microbiol, 165 (7): 481–489

Zhou Ke, Pan Hongmiao, Zhang Shengda, et al. 2011. Occurrence and microscopic analyses of multicellular magnetotactic prokaryotes from coastal sediments in the Yellow Sea. Chin J Oceanol Limnol, 29(2): 246–251

Zhou Ke, Zhang Wenyan, Pan Hongmiao, et al. 2013. Adaptation of spherical multicellular magnetotactic prokaryotes to the geochemically variable habitat of an intertidal zone. Environ Microbiol, 15(5): 1595–1605

Zhou Ke, Zhang Wenyan, Yuzhang K, et al. 2012. A novel genus of multicellular magnetotactic prokaryotes from the Yellow Sea. Environ Microbiol, 14(2): 405–413

Zhu Kailing, Pan Hongmiao, Li Jinhua, et al. 2010. Isolation and characterization of a marine magnetotactic spirillum axenic culture QH-2 from an intertidal zone of the China Sea. Res Microbiol, 161(4): 276–283

Appendix:

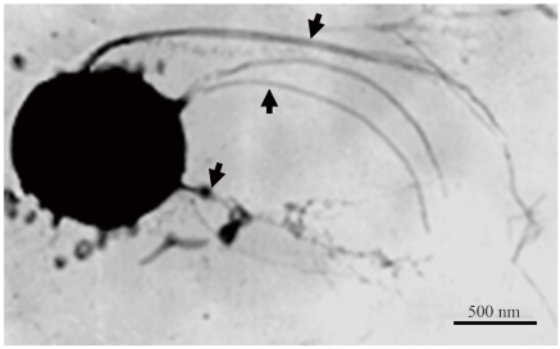

Fig. A1. The cocci with three flagella bundles (black arrows).

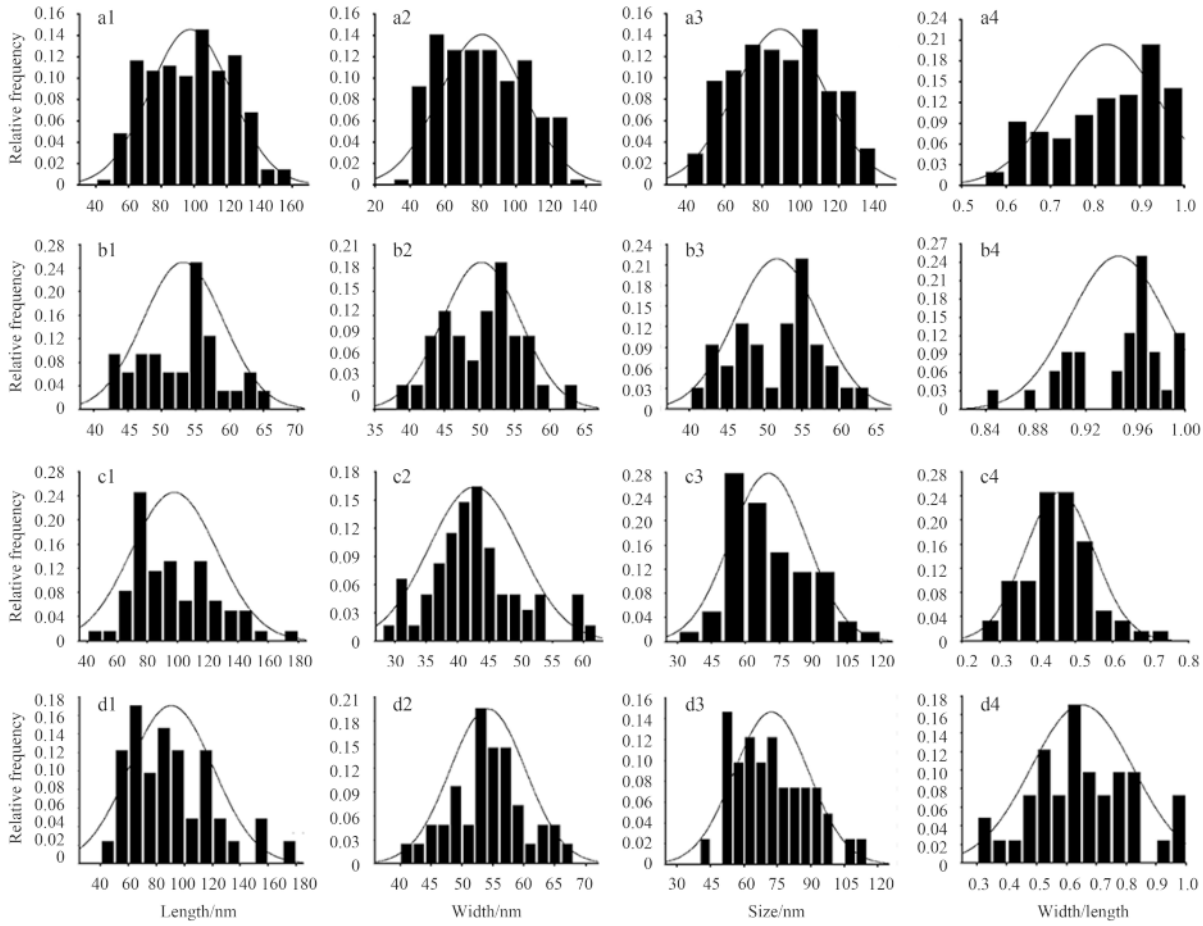

Fig. A2. Histograms of the length (d1), width (d2), size (d3) and width/length ratio (d4) of the magnetosomes. a1–a4. Prismatic magnetosomes in magnetococci, b1–b4. cubo-octahedral magnetosomes, c1–c4. bullet-shaped magnetosomes, and d1–d4. tooth- or flake-shaped magnetosomes.

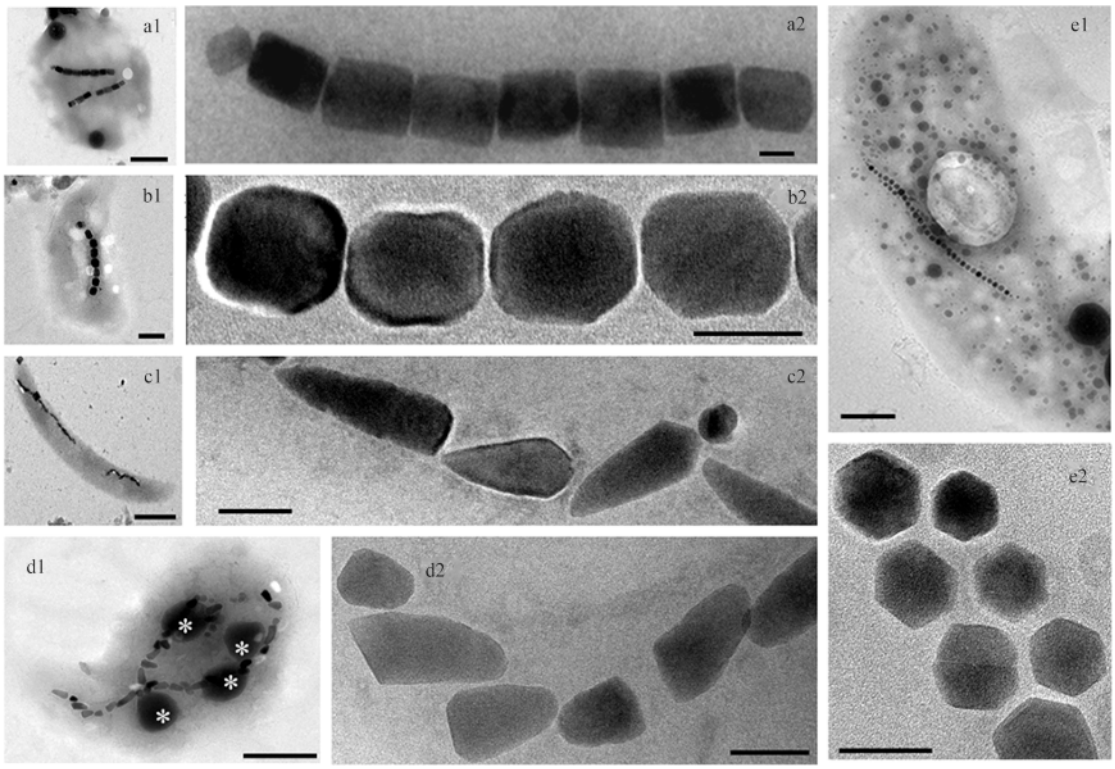

Fig. A3. TEM images showing the morphology of magnetosomes. a1 and a2. Prismatic magnetosomes in magnetococci, b1 and b2. prismatic magnetosomes in vibrio MTB, c1 and c2. Bullet-shaped magnetosomes in rod-shaped MTB, d1 and d2. tooth-or flake-shaped magnetosomes in handle-shaped MTB, and e1 and e2. cubo-octahedral magnetosomes in vibrio MTB. Scale bars are 500 nm in Panels a1, b1, c1, d1, e1 and 50 nm in the other panels.

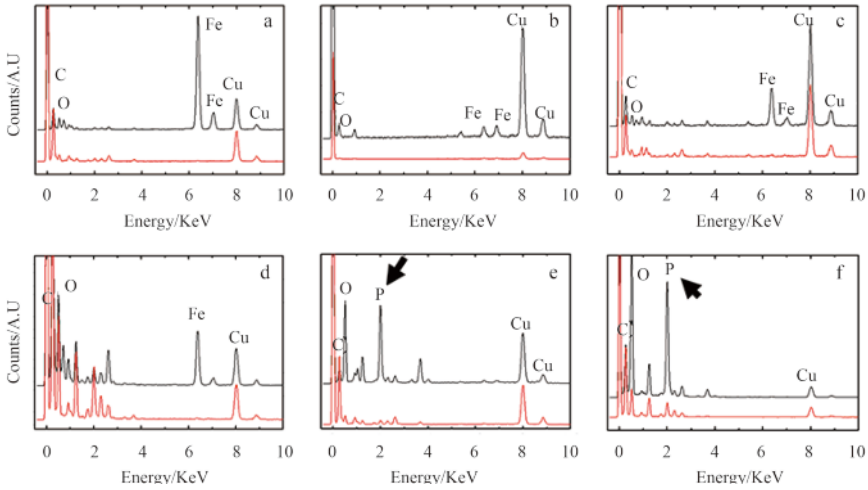

Fig. A4. EDXS analysis of the magnetosomes and cell inclusions. a. Prismatic magnetosomes in Fig. 2a1, b. cubo-octahedral magnetosomes in Fig. 2h1, c. bullet-shaped magnetosomes in Fig. 2k1, and d. tooth- or flake-shaped magnetosomes in Fig. 2l1. The graphs revealed peaks for iron and oxygen and the copper TEM grid explains the peak for copper. Red line represents cell and black line magnetosome. e and f. The EDXS analysis of the dense black granules (*) in Fig. 2d and l, respectively. The black arrow shows the peak of phosphorus and the copper TEM grid explains the peak for copper. Red line represents cell and black line dense granules.